NACA RM A57KO7a

NACA

RESEARCH MEMORANDUM

HEAT TRANSFER ON AN AFTERBODY IMMERSED IN THE SEPARATED WAKE OF A HEMISPHERE

By Helmer V. Nielsen

Ames Aeronautical Laboratory
Moffett Field, Calif.

NATIONAL ADVISORY COMMITTEE
FOR AERONAUTICS
WASHINGTON

January 30, 1958
Declassified February 8, 1960

NATIONAL ADVISORY COMMITTEE FOR AERONAUTICS

RESEARCH MEMORANDUM

HEAT TRANSFER ON AN AFTERBODY IMMERSED IN THE SEPARATED WAKE OF A HEMISPHERE

By Helmer V. Nielsen

SUMMARY

Tests were conducted to determine the average heat transfer and temperature recovery factor on a tapered cylindrical afterbody immersed in the wake of a hemisphere. The range of the investigation was from a Reynolds number of 125,000 to 870,000 (based on hemisphere diameter and free-stream conditions). The nominal Mach number was 2.4.

At the lower end of the Reynolds number range, the average heat transfer (as represented by the Stanton number) from the afterbody was approximately half that from the hemisphere whether the boundary layer being separated from the rear edge of the hemisphere was turbulent or transitional. As the Reynolds number was increased, the Stanton number for both the hemisphere and the afterbody decreased but at a greater rate for the afterbody. The slope of the afterbody curve indicates that the heat-transfer coefficient was nearly independent of pressure level over the range tested.

The temperature recovery factor for the afterbody (based on free-stream conditions) was slightly lower than that for the nose whether the separated boundary layer was turbulent or transitional. The numerical values were approximately 0.89 for the nose and from 0.82 to 0.87 for the afterbody.

INTRODUCTION

As higher and higher Mach numbers are contemplated the problem of aerodynamic heating assumes increasing importance. Many physical schemes and geometrical configurations have been proposed to alleviate this problem. It is the purpose of the present paper to report on a wind-tunnel investigation of one such device, the use of a separated boundary layer from the nose section of a body to protect the aftersection.

NOTATION

A	surface area, sq ft
BL	boundary layer
C_p	specific heat of air at constant pressure
d	diameter of hemisphere, ft
h	average heat-transfer coefficient, Btu/hr, sq ft, ^{o}F
M	Mach number
Q	heat rate, Btu/hr
q	specific heat rate, Btu/hr, sq ft
Re	Reynolds number, $\frac{V_\infty \rho_\infty d}{\mu_\infty}$
r	temperature recovery factor, $\frac{T_r - T_\infty}{T_t - T_\infty}$
St	Stanton number, $\frac{h}{\rho_\infty V_\infty C_{p_\infty}}$, dimensionless
T	temperature, ^{o}F abs
V	velocity, ft/sec
ρ	mass density, slugs/cu ft
μ	viscosity, lb-sec/sq ft

Subscripts

a	conditions on the afterbody section of model
n	conditions on the nose section
r	recovery conditions

t stagnation conditions

∞ free-stream conditions

DESCRIPTION OF EQUIPMENT

Wind Tunnel

This investigation was conducted in the Ames 6-inch heat transfer wind tunnel which is described in detail in reference 1. This wind tunnel has replaceable nozzle blocks and for the present investigation those providing a nominal Mach number of 2.4 were used.

Model

The model consisted of two copper segments, a hemispherical nose 1.250 inches in diameter and a truncated conical afterbody one half the nose diameter in length (0.625 in.), with a base diameter of 0.875 inch and a cone half-angle of 21° (fig. 1). These two segments were mounted in the wind tunnel by means of a hollow Micarta sting which kept them thermally and electrically isolated. Preliminary estimates of the maximum possible conduction showed that the heat leakage along the Micarta sting was less than 1 percent. An additional precaution exercised to prevent heat leakage from one part to the other was to provide a small air gap between the segments at their common boundary.

Both sections were heated independently by means of small 30-watt electrical heaters. These heaters were fabricated by winding electrically insulated constantan wire around small copper cylinders which were then inserted in the respective segments of the model. The front heater was screwed into place while the rear heater was cemented with a ceramic heat-conducting cement. Three Nichrome V - constantan thermocouples were imbedded in the nose, two in the afterbody, and five more along the support shafts.

TEST PROCEDURE

Average heat-transfer rates and recovery temperatures were obtained by measuring heater resistances, current inputs, body temperatures, and wind-tunnel stagnation temperatures. The tests were conducted at Mach numbers ranging from 2.35 to 2.42, the nominal Mach number was 2.4. The Reynolds number, based on nose diameter and free-stream conditions, ranged from approximately 125,000 to 870,000.

The method used in conducting the tests was to balance the temperatures between the two sections. At each pressure level (Reynolds number) tested, the heat input to the nose was varied in six approximately equal steps from 0 to a maximum of 30 watts. At each heat input level the afterbody was raised to the same temperature as the nose to eliminate heat conduction between the two. The temperatures and power inputs were then recorded.

In order to enable qualitative studies of flow patterns and wake angles, shadowgraphs were also taken during the test runs.

DATA REDUCTION

Average heat-transfer coefficients and average recovery temperatures were found from the equation

$$Q = hA(T - T_r) \tag{1}$$

by the method of least squares using the six different sets of measured values of heat input and body temperature. An equivalent graphical method is to plot Q/A as a function of T for each section of the body. In the range of temperatures tested (50° F to 200° F) the heat-transfer coefficient was independent of the body temperature and thus equation (1) formed a straight line with h as the slope and T_r (the recovery temperature) as the intercept where $Q/A = 0$.

DISCUSSION OF RESULTS

The heat-transfer results for the smooth forebody are presented in figure 2 in the form of Stanton number as a function of Reynolds number, all based on properties behind a normal shock wave. Since the frontal area of the forebody is a hemisphere the heat transfer from this area should correlate with known hemisphere data, for example, references 2 and 3. With this end in view, estimates of the heat lost from the rear of the forebody were made on the assumption that the rearward facing annulus of the nose had the same heat-transfer coefficient and recovery temperature as the afterbody. These estimates were then subtracted from the total heat transferred and the results were plotted with the data of references 2 and 3. It can be seen from figure 2 that they are in good agreement with the previous results which, incidentally, represent two separate models and a wide range of Mach numbers.

Figure 3 also shows the heat transfer from the smooth forebody in the form of Stanton number as a function of Reynolds number, this time, however, based on free-stream properties. The dimensions used were the

diameter and the area of the hemispherical surface, respectively. The area of the exposed rearward facing annulus was not used; so if it is desired to express the Stanton numbers in terms that include this surface, it is necessary to multiply the values of figure 3 by an appropriate area ratio. In the present case that ratio has a numerical value of 0.796.

Primarily, the purpose of figure 3 is to exhibit the afterbody results which, like the forebody results, are based on free-stream properties. It can be seen that when the nose was smooth it was not possible to draw a straight line through the afterbody data points. Shadowgraphs, typical examples of which are shown in figure 4, showed that transition from laminar to turbulent flow was occurring in the boundary layer after it separated from the afteredge of the forebody, except for the two lowest Reynolds numbers where transition appeared to occur at the separation point. The transition point was not stationary but appeared to oscillate about some mean position. In addition, this mean position seemed to move downstream with increase in Reynolds number up to approximately 770,000, at higher Reynolds numbers it moved upstream again. Customarily the transition point moves progressively upstream with Reynolds number; this would alter the variation of Stanton number with Reynolds number from that shown in figure 3. However, this figure does illustrate the difference in heat transfer between turbulent and transitional separated boundary layers.

In order to fix transition on the forebody the nose was coated with No. 180 Carborundum grit and the tests were repeated. These results are also shown in figure 3 and it can be seen that they are in good agreement with the data of Crawford and Rumsey (ref. 4) who tested a very similar model although at a slightly lower Mach number. It should be noted that the straight line drawn through the data points has a negative slope of approximately 1. The significance of this is not immediately apparent but writing out the equation represented by this line reveals that the heat-transfer coefficient was nearly independent of pressure level. This is not characteristic of heat-transfer coefficients with attached boundary layers and may be caused by the following process: The resistance to heat transfer from the afterbody can be thought of as the sum of two parts, the thermal resistance of the separated boundary layer and the thermal resistance of the wake in which the afterbody is immersed. If the resistance in the wake region is much greater than in the separated boundary layer and if, furthermore, this resistance is governed by the thermal conductivity of air or by some mixing mechanism which is relatively independent of pressure, results such as the foregoing could conceivably be obtained. However, one would intuitively expect that the mass transfer or "mixing" across the boundary layer would be pressure dependent. Therefore, investigation of local flow properties would be necessary before a definitive explanation could be given. Unfortunately, this is beyond the scope of the present work and beyond the capabilities of the present model.

It should be noted that the Stanton numbers for the transitional separated boundary layer are higher than for the completely turbulent boundary layer. This could conceivably be caused by increased activity in the boundary layer (i.e., the oscillation of the transition point) affecting the mixing in the wake. A similar increase in heat transfer at transition in an attached boundary layer on a flat plate has previously been noted by Slack (ref. 5).

Temperature recovery factors are presented in figure 5. They were obtained from the average recovery temperature as found from the zero intercept of the Q versus T curve, that is, by extrapolating to the condition of zero net heat transfer. It should be noted that the average recovery factor found by this method differs from the value that would be found from averaging the local values of recovery factor over the surface of the body. It also differs from one that would be found from the condition of zero heat input to both bodies. In that case the net heat transfer from each of the bodies would not be zero; that is, heat would be transferred from one body to the other through the wake.

The temperature recovery factor for the afterbody was slightly lower than for the nose in both the transitional and the completely turbulent cases and decreased slightly with increasing Reynolds number. The approximate numerical values were 0.89 for the nose and from 0.82 to 0.87 for the afterbody.

Throughout this discussion it should be kept in mind that the presence of the support sting prevents the data from being truly representative of free-flight conditions. Although the sting diameter was as small as possible, it still blocked off the entire base area of the afterbody from the air stream. However, preliminary tests with dummy models and support shafts varying in diameter from 3/16 to 3/8 inch showed no differences in wake angles or shock-wave patterns. This is in accordance with results observed by Chapman in reference 6 where at comparable Mach numbers little effect on base pressure was noted for support to base diameter ratios up to 0.6. Similarly, the effects of support length were found to be negligible when the ratio of length to base diameter was over 2.8. In the present case the ratio is either 2.85 or 3.35 depending on whether or not the afterbody length is included.

Ames Aeronautical Laboratory
National Advisory Committee for Aeronautics
Moffett Field, Calif., Nov. 7, 1957

REFERENCES

1. Stalder, Jackson R., Rubesin, Morris W., and Tendeland, Thorval: A Determination of the Laminar-, Transitional-, and Turbulent-Boundary-Layer Temperature-Recovery Factors on a Flat Plate in Supersonic Flow. NACA TN 2077, 1950.

2. Stalder, Jackson R., and Nielsen, Helmer V.: Heat Transfer from a Hemisphere-Cylinder Equipped with Flow-Separation Spikes. NACA TN 3287, 1954.

3. Stalder, Jackson R., and Inouye, Mamoru: A Method of Reducing Heat Transfer to Blunt Bodies by Air Injection. NACA RM A56B27a, 1956.

4. Crawford, Davis H., and Rumsey, Charles B.: Heat Transfer in Regions of Separated and Reattached Flows. NACA RM L57D25b, 1957.

5. Slack, Ellis G.: Experimental Investigation of Heat Transfer Through Laminar and Turbulent Boundary Layers on a Cooled Flat Plate at a Mach Number of 2.4. NACA TN 2686, 1952.

6. Chapman, Dean R.: An Analysis of Base Pressure at Supersonic Velocities and Comparison with Experiment. NACA Rep. 1051, 1951. (Supersedes NACA TN 2137).

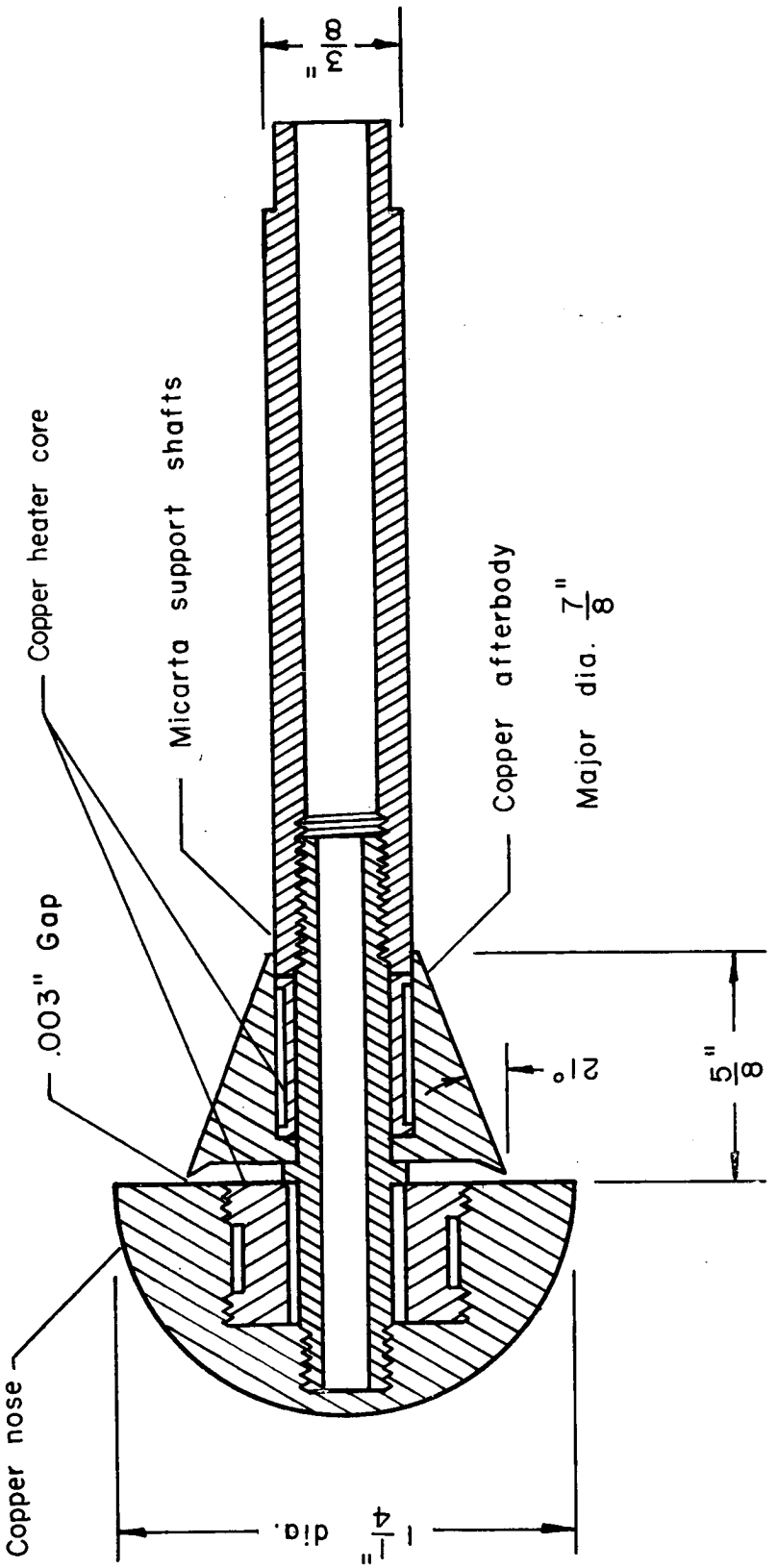

Figure 1.- Section view of wake separation model.

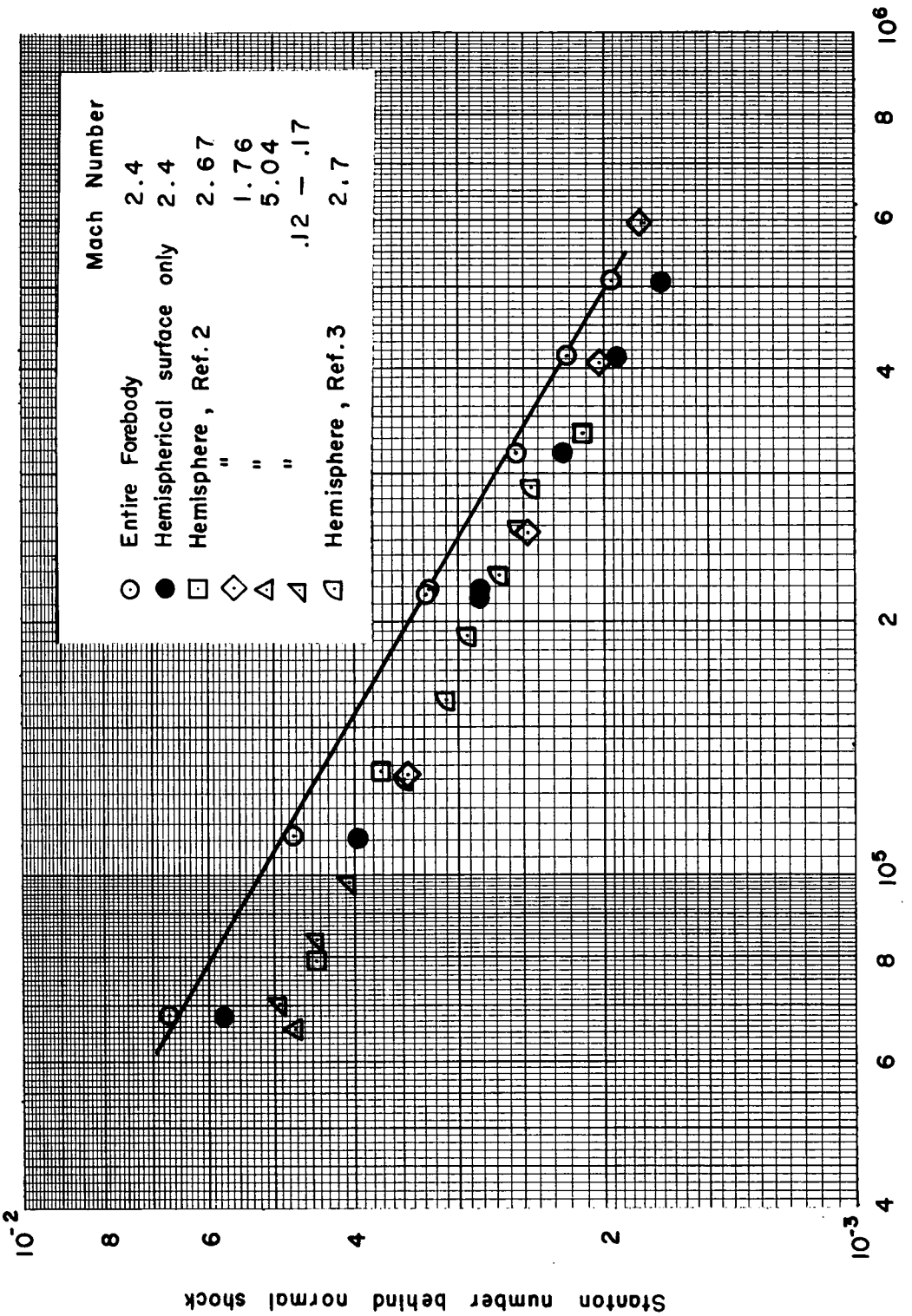

Figure 2.- Correlation of data based on properties behind a normal shock wave.

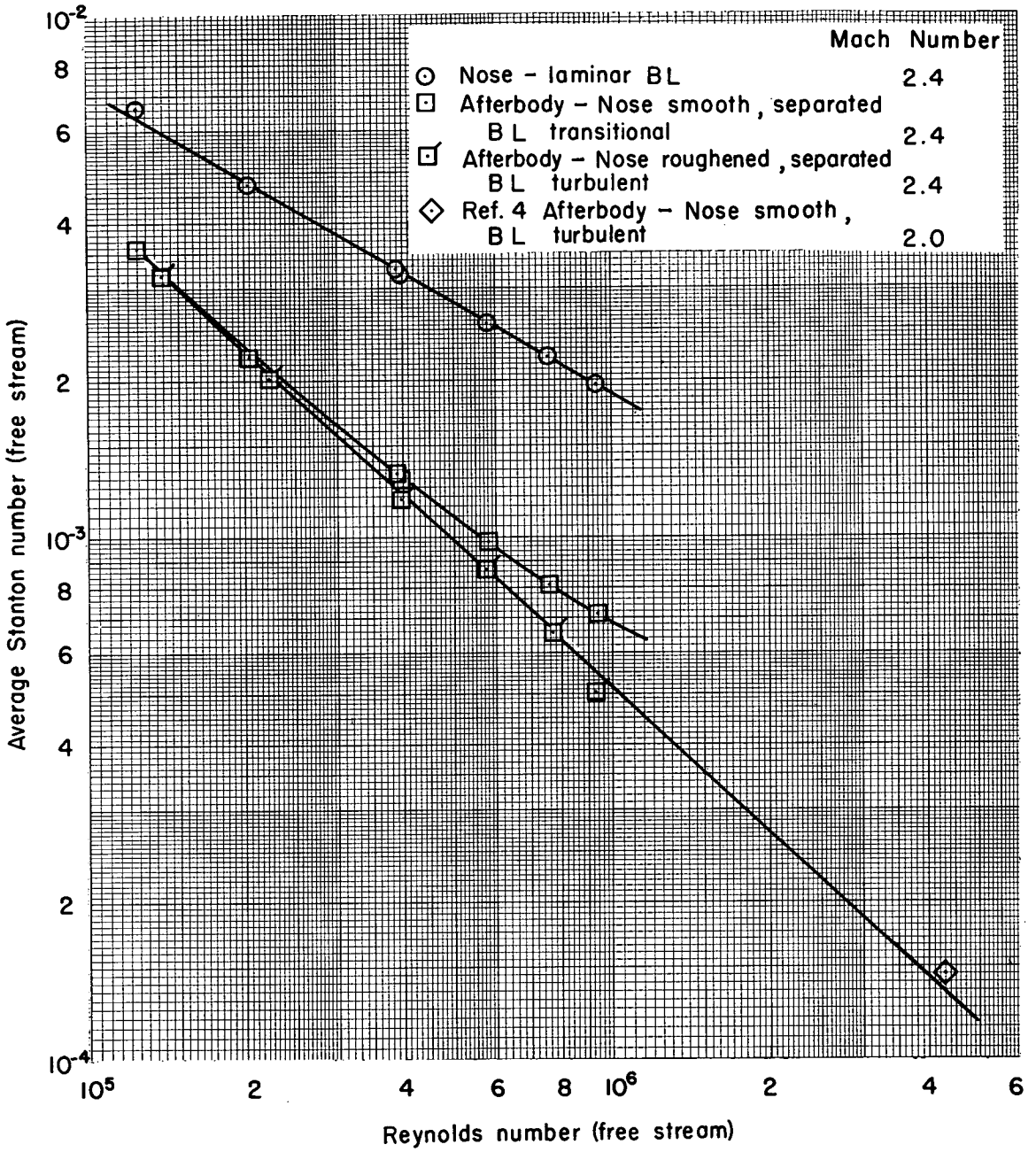

Figure 3.- Average heat transfer in a separated wake.

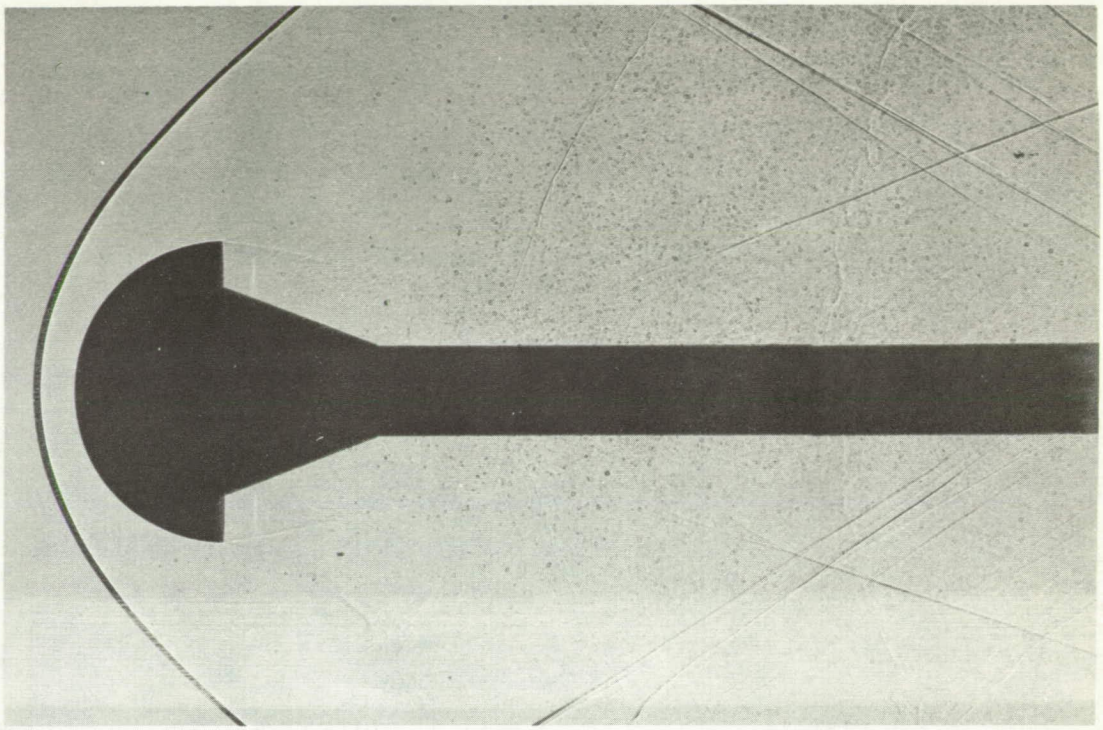

(a) Transitional boundary layer; nose smooth. A-22786

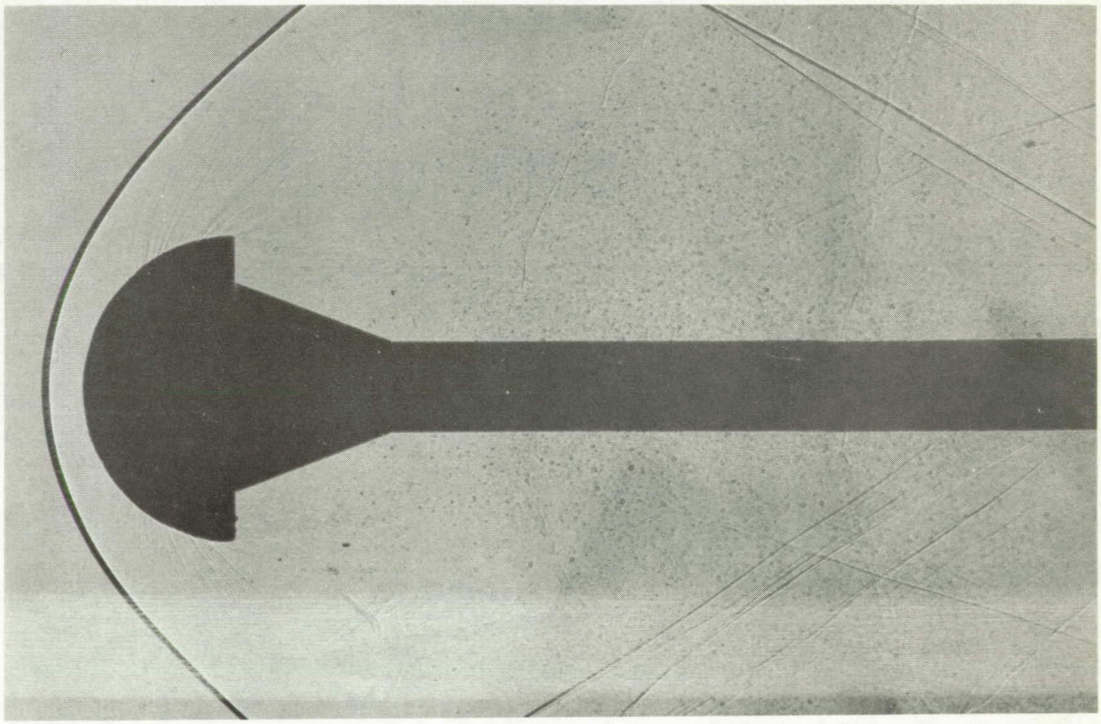

(b) Turbulent boundary layer; nose roughened. A-22787

Figure 4.- Shadowgraphs of wake separation model at $M = 2.4$; $Re = 9.35 \times 10^5$.

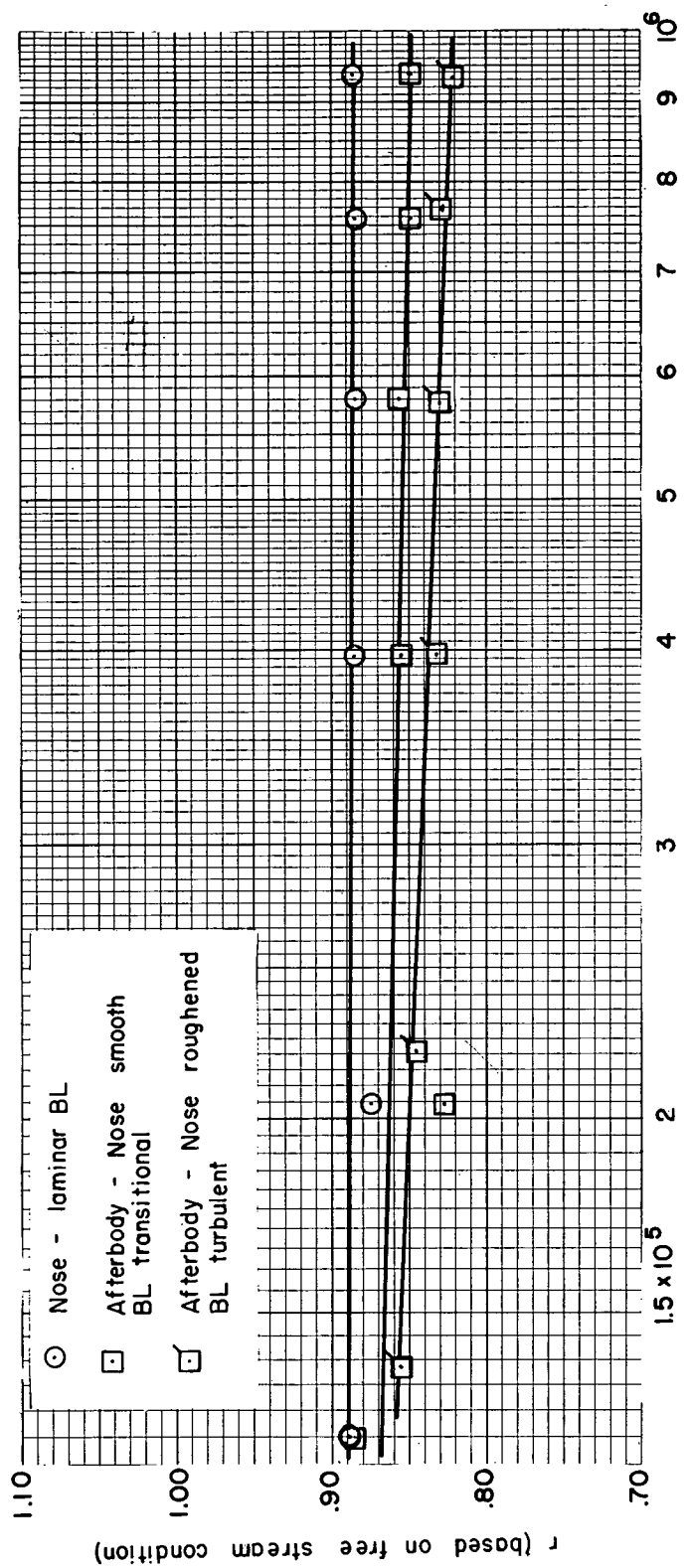

Figure 5.- Average temperature recovery factor on nose and afterbody of separated wake model.